

Finding Lead Compounds for Dengue Antivirals from a Collection of Old Drugs through *In Silico* Target Prediction and Subsequent *In Vitro* Validation

Zafirah Liyana Abdullah, Hui-Yee Chee, Rohana Yusof, and Fazlin Mohd Fauzi*

Cite This: *ACS Omega* 2023, 8, 32483–32497

Read Online

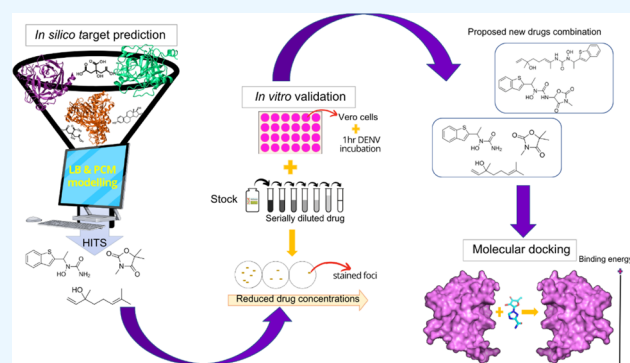
ACCESS |

Metrics & More

Article Recommendations

Supporting Information

ABSTRACT: Dengue virus (DENV) infection is one of the most widely spread flavivirus infections. Despite the fatality it could cause, no antiviral treatment is currently available to treat the disease. Hence, this study aimed to repurpose old drugs as novel DENV NS3 inhibitors. Ligand-based (L-B) and proteochemometric (PCM) prediction models were built using 62,354 bioactivity data to screen for potential NS3 inhibitors. Selected drugs were then subjected to the foci forming unit reduction assay (FFURA) and protease inhibition assay. Finally, molecular docking was performed to validate these results. The *in silico* studies revealed that both models performed well in the internal and external validations. However, the L-B model showed better accuracy in the external validation in terms of its sensitivity (0.671). In the *in vitro* validation, all drugs (zileuton, trimethadione, and linalool) were able to moderately inhibit the viral activities at the highest concentration tested. Zileuton showed comparable results with linalool when tested at 2 mM against the DENV NS3 protease, with a reduction of protease activity at 17.89 and 18.42%, respectively. Two new compounds were also proposed through the combination of the selected drugs, which are ziltri (zileuton + trimethadione) and zilool (zileuton + linalool). The molecular docking study confirms the *in vitro* observations where all drugs and proposed compounds were able to achieve binding affinity ≥ -4.1 kcal/mol, with ziltri showing the highest affinity at -7.7 kcal/mol, surpassing the control, panduratin A. The occupation of both S1 and S2 subpockets of NS2B-NS3 may be essential and a reason for the lower binding energy shown by the proposed compounds compared to the screened drugs. Based on the results, this study provided five potential new lead compounds (ziltri, zilool, zileuton, linalool, and trimethadione) for DENV that could be modified further.



1. INTRODUCTION

Dengue is a mosquito-borne viral disease where the primary mode of transmission of dengue virus (DENV) between humans involves the *Aedes aegypti* mosquito as the primary vector, with *Aedes albopictus* as the secondary vector. These two vectors have caused viral endemic in more than 100 countries including Eastern Mediterranean, American, South-East Asian, Western Pacific, and African regions. According to the World Health Organization (WHO), the prevalence of dengue infection has increased eightfold in the last two decades, with reported deaths increasing from 960 to 4032, between the years 2000 and 2015.¹ As of June 2022, 849 death has been recorded worldwide.² In general, dengue infection typically presents as an acute febrile illness accompanied by headaches, retro-orbital pain, arthralgia, and myalgia. Although the majority of dengue cases are either asymptomatic or mild, a large number of cases develop into potentially life-threatening severe diseases, such as dengue hemorrhagic fever (DHF) and dengue shock syndrome (DSS).³ Moreover, life-threatening

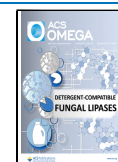
conditions increase when infection occurs in individuals with asthma, diabetes, and other chronic illness.

Despite the urgency to combat the disease, no effective treatment is yet available in the market. The current treatment only involves supportive care in the form of fluid therapy and close clinical monitoring. One preventive treatment, the vaccine Dengvaxia, was approved in 2019 by the U.S. Food and Drug Administration (FDA).⁴ However, the vaccine efficacy is varied by age, the DENV serotype that causes the infection, and the serostatus of the vaccine recipient.⁵ Therefore, an efficient antiviral agent to treat DENV infection is urgently needed. A DENV antiviral treatment should inhibit all dengue serotypes⁶ and be administered to patients with or

Received: April 16, 2023

Accepted: July 14, 2023

Published: August 28, 2023



without a fever to decrease or prevent disease symptoms at the first sign of dengue infection, thus decreasing the risk of severe dengue diseases.

Understanding the life cycle of dengue virus reveals the potential targets for anti-dengue, and these include proteins involved in events such as endocytosis, viral fusion to the host membrane, viral transcription, and the release of progeny viruses from the host cell.⁷ Among these, the NS3 protein is an interesting target for potential antiviral development. This protein is among the best-characterized DENV nonstructural proteins and is the most preserved in all dengue virus serotypes.⁸ The NS3 protease, composed of NS2B and NS3, is a vital component in the replication cycle of the dengue virus. It acts as a trypsin-like serine protease, with His51, Asp75, and Ser135 as its key components.⁸ The NS3 protease plays a crucial role in cleaving the viral polyprotein at various sites, including NS2A-NS2B, NS2B-NS3, NS3-NS4A, and NS4B-NS5.⁸ Hence, the disturbance of the NS3 protease is fatal to the virus, therefore can be considered a useful target for antiviral drugs.⁹ Several studies have shown the promising result of inhibitors targeting DENV NS3.^{10,11} In fact, a similar target was successfully used for Hepatitis C virus (HCV) treatment.¹²

The use of “old drugs” and compounds available in the databases may accelerate the discovery of anti-dengue NS3 inhibitors, and *in silico* approaches provide systematic understandings of complex relationships among drugs, targets, and diseases essential for successful repositioning.¹³ In addition, the availability of well-curated compounds databases, as well as the advancement of machine learning, offer unprecedented opportunities to conduct drug repositioning. There are three *in silico* methods that can be used for this purpose, which are ligand-based, structure-based, and proteochemometric (PCM) modeling. The ligand-based (L-B) method utilizes the structural information of compounds. Using suitable descriptors, the functional relationships between compounds in a data set and one or more known actives are examined, usually through machine learning algorithms. The structure-based method uses the structural information of the target receptor. Here, the method predicts the preferred pose of ligands in the binding site through the use of scoring functions. The PCM method, on the other hand, predicts the bioactivity by using information from both compounds and target receptors.

Hence, this study aims to discover lead compounds of DENV NS3 inhibitors from a collection of “old drugs” and substances through two different *in silico* target predictions, which are L-B and PCM models. Consequently, the results of the target prediction were validated through *in vitro* validation, which involves the foci forming reduction assay (FFURA) and NS3 protease assay. In FFURA, the antiviral properties of the drugs were evaluated on the dengue-infected Vero cells, while the protease assay was performed to measure drug inhibition toward the NS3 protease activity. From the *in vitro* observation, two new compounds were proposed, which were developed from the combinations of the selected drugs. Finally, molecular docking was conducted on the selected drugs and the proposed compounds to observe the interaction that was involved in the formation of the drug–protein complex.

2. RESULTS

2.1. *In Silico* Prediction of Lead Compounds for the Anti-Dengue NS3 Inhibitor Using Ligand-Based (L-B)

and Proteochemometric (PCM) Prediction Models.

2.1.1. Internal Validation of Predictive L-B and PCM Models.

Table 1 shows the internal validation of the two models, where

Table 1. Internal Validation of the Training Set^a

model	λ	TP	FP	TN	FN	SEN	SPE
PCM	0.8	18,948	3174	36,881	3351	0.850	0.921
	0.83	18,946	3172	36,883	3353	0.850	0.921
	0.86	18,945	3172	36,883	3354	0.850	0.921
	0.89	18,945	3172	36,883	3354	0.850	0.921
	0.92	18,945	3172	36,883	3354	0.850	0.921
	0.95	18,944	3172	36,883	3354	0.850	0.921
	0.98	18,944	3172	36,883	3354	0.850	0.921
	L-B		18,697	672	39,364	3621	0.838

^aFor the PCM model, the evaluation was conducted for the lambda value ($\lambda = 0.8, 0.83, 0.86, 0.89, 0.9, 0.93, 0.96, \text{ and } 0.99$). TP—true positive, FP—false positive, TN—true negative, FN—false negative, SEN—sensitivity, SPE—specificity.

sensitivity and specificity were used as performance measures. Both models scored almost similar values in terms of sensitivity and specificity. However, the PCM model scored a slightly higher sensitivity than L-B (0.85 vs. 0.838) but lower specificity than L-B (0.921 vs. 0.983). Note that the performance of PCM plateaued and did not change with the increasing lambda value. Hence, 0.8 was considered the best lambda value for the PCM model. We placed higher importance on models with higher sensitivity as the focus is more on identifying active compounds (TP) than inactive compounds (TN). In this case, the PCM model showed better performance in the internal validation compared to the L-B model.

2.1.2. External Validation of Predictive L-B and PCM Models. Table 2 summarizes the result of the external

Table 2. External Validation to Assess the Performance of PCM and L-B Models^a

model	TP	FP	TN	FN	sensitivity	specificity
PCM	1121	3168	13,570	961	0.538	0.811
L-B	1393	5345	11,399	683	0.671	0.681

^aTP—true positive, FP—false positive, TN—true negative, FN—false negative, SEN—sensitivity, SPE—specificity.

validation for both PCM and L-B models. As mentioned, a lambda value of 0.8 was considered the best and hence was used in the external validation and screening exercise for PCM. It can be seen that the L-B model showed a higher sensitivity than PCM (0.671 vs. 0.538) but showed a lower specificity than PCM (0.681 vs. 0.811). This indicates that the L-B model is better at predicting active compounds, whereas PCM is better at predicting inactive compounds. Overall, we deduced that the L-B model performs better compared to the PCM model, as a higher sensitivity score is preferable in the current study, and external validation has more weightage than internal validation as external validation measures the ability of the model to predict instances it has never encountered before.

The applicability domain was measured using leverage and similarity search for each compound. Here, the leverage value and similarity search were calculated for each compound in the external data set against each compound in the training set. The results of both methods are presented in Figure 1. Here, only 1.69% of compounds from the test set were predicted as

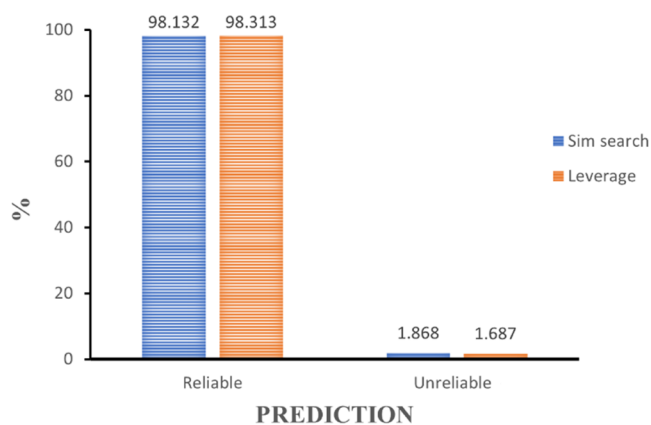


Figure 1. Applicability domain (AD) using similarity search and leverage. Based on the score, both algorithms show that the model reliably predicts the test set activity. Analyses were conducted using the Knime⁴⁵ Analytics Platform.

unreliable from the leverage nodes and 1.87% from the similarity search nodes. Looking at the high leverage score and similarity search (>98%), it can be deduced that the result of the validation is valid as the high sensitivity and specificity values were corroborated by the result of the applicability domain. In addition, the chemical space covered by the predictive model was also determined using principal component analysis (PCA) (see Supporting Information S1). It was found that the chemical space covered by the external set falls within the boundaries of the chemical space of the training set and hence is deemed to be within the applicability domain of the constructed model.

2.1.3. Screening of “Old” Drugs as the Potential DENV NS3 Inhibitor. In the drug screening process, a total of 1263 drugs were collected from SWEETLEAD¹⁴ and DrugBank.¹⁵ Out of the whole drug set, 16 drugs from the PCM model (score ≥ 0.99) and two drugs from the L-B model (score ≥ 0.5) were identified. From the PCA plot, it was found that most of the drugs predicted using the PCM model lie within the training set boundaries, while the drugs predicted using the RF modeling lie close to the compounds but not in the heavily populated area (see the Supporting Information, Figure S2). The list of the drugs is presented in Tables 3 and 4. For *in vitro* validation purposes, not all drugs were used for further testing. Only three drugs were selected from the screening, which were zileuton, trimethadione (from the PCM model), and linalool (L-B model). Zileuton and trimethadione were selected as they were located at the center of the PCA graph, which indicated a highly populated area of the active inhibitor in the training set. Linalool was selected as it is closer to the highly populated area, as compared to the sesame. This signifies a high similarity with the training set. Additionally, the availability of the literature, specifically on *in vitro* studies of these drugs, was also taken into consideration.

2.2. In Vitro Validation of the Selected Drugs as Anti-Dengue NS3. **2.2.1. Drugs Cytotoxicity on Vero Cells.** The drugs that were selected for *in vitro* validation were initially tested for cytotoxicity effect. In general, all drugs exhibited low cellular toxicity in Vero cells, even at a millimolar concentration, as indicated in Figure 2. The first drug, zileuton, was tested in the range of concentrations between 0.25 to 4 mM. A concentration of 4 mM was set as the highest concentration allowed to maintain the solvent concentration at

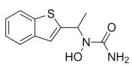
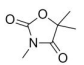
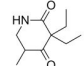
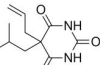
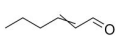
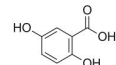
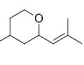
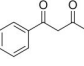
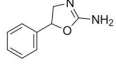
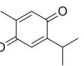
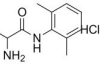
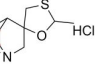
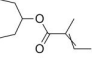
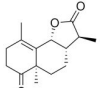
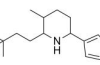
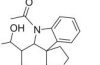
1% v/v. After 72 h of incubation, all tested concentrations, 0.25, 0.5, 1, 2, and 4 mM showed cell viability above 80%. The calculated 50% cytotoxic concentration (CC_{50}) value was 38.67 mM. Next, trimethadione was tested in the range of 1.25–20 mM. The drug showed a dose-dependent response where, as the concentration increased, the percentage of cell viability was also reduced. However, at the highest tested concentration of 4 mM, the cells maintained its viability at 80%. Based on the analysis, the calculated CC_{50} of trimethadione was 117 mM. The third drug, linalool, was tested in the range of 0.125–2 mM. A concentration of 2 mM was used as the highest concentration to maintain the solvent concentration at 1% v/v. After 72 h of incubation, cells tested at different concentrations of 0.125, 0.25, 0.5, 1, and 2 mM maintained more than 80% of cell viability, with calculated CC_{50} value was 17.47 mM. Lastly, the positive control, ribavirin, maintained its cell viability above 90%, even at the highest concentration of 1 mM. The CC_{50} value calculated by GraphPad for ribavirin was 49 mM. The cytotoxicity of the solvent of the drugs, which is ethanol, on the cells was also studied here. Here, the highest solvent percentage tested is up to 2% v/v, with cell viability at 86%.

2.2.2. Anti-Dengue Activities of Selected Drugs on Infected Vero Cells. To test the inhibitory potential of the drugs on the infected cell, similar drug concentration, which was confirmed safe to be used *via* the cytotoxicity test, were used. After an hour of viral incubation, the dengue virus was expected to penetrate the host cell and begin its replication and reproduction by using the host's cellular metabolism, and later, a fully formed virus will be assembled. After 72 h, the infected cells were incubated with tested drugs, where the end-point assay was conducted and resulted in the formation of brown-colored localized clusters called foci. Figure 3 is the results of infected Vero cells, which have been treated with the drugs zileuton, trimethadione, linalool, and ribavirin (positive control).

Based on the results, all treatments showed a dose-dependent response trend where foci reduction increases with increasing drug concentration. For zileuton, it showed the highest foci reduction with an average of 47% at the highest concentration tested, 4 mM. Although dose–response trend can be seen from the result; however, there are slight differences in the trend between the inhibition of foci at 1 and 2 mM, where at 2 mM, zileuton caused slightly lower foci inhibition compared to the treatment of 1 mM. The projected half-maximal inhibitory concentrations (IC_{50}) value calculated was 3.3 mM. For trimethadione, the highest foci inhibition (36%) was recorded at 20 mM. The calculated IC_{50} for trimethadione was 25.97 mM. Among the tested drugs, only linalool demonstrated foci reduction above 50%, where the highest foci inhibition (54%) was observed at 2 mM. The IC_{50} calculated for linalool was 1.12 mM. Looking at the presented data, it should be noted that none of the selected drugs showed a better antiviral effect than the ribavirin in terms of the concentration used to achieve a 50% foci reduction. Based on the assay, the calculated IC_{50} for ribavirin was 0.14 mM which was the lowest among the four drugs. Ribavirin also showed 88% foci inhibition at the highest concentration tested, 1 mM.

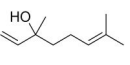
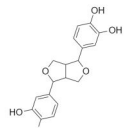
2.2.3. DENV-2 NS2B-NS3pro Inhibition by Selected Drugs. Figure 4 shows the protease inhibition of the drugs. In terms of protease inhibition, the positive control, aprotinin, performed the best against the selected drugs and ribavirin. Aprotinin, the positive control for this assay, is a competitive serine protease

Table 3. List of Drugs/Substances Screened and Filtered from PCM and Its Indication^a

#	Name	Chemical structure	Indication	Remarks	Score
1	Zileuton		For the prophylaxis and chronic treatment of asthma in adults and children 12 years of age and older ¹⁴ .	Stimulate numerous biological effects including augmentation of neutrophil and eosinophil migration, neutrophil and monocyte aggregation, leukocyte adhesion, increased capillary permeability, and smooth muscle contraction ¹⁴ .	0.999
2	Trimethadione		Used in the control of absence (petit mal) seizures that are refractory to treatment with other medications ¹⁴ .	Dione anticonvulsants reduce T-type calcium currents in thalamic neurons, including thalamic relay neurons ¹⁴ .	0.999
3	Methyprrylon		For the treatment of insomnia ¹⁴ .	Methyprrylon binds at a distinct binding site associated with a Cl ⁻ ionopore at the GABA _A receptor, increasing the duration of time for which the Cl ⁻ ionopore is open ¹⁴ .	0.999
4	Butalbital		Used in combination with acetaminophen or aspirin and caffeine for its sedative and relaxant effects in the treatment of tension headaches, migraines, and pain ¹⁴ .	Butalbital binds at a distinct binding site associated with a Cl ⁻ ionopore at the GABA _A receptor, increasing the duration of time for which the Cl ⁻ ionopore is open ¹⁴ .	0.999
5	Hexenal		For the induction of anesthesia prior to the use of other general anesthetic agents and for induction of anesthesia for short surgical, diagnostic, or therapeutic procedures associated with minimal painful stimuli ¹⁴ .	Hexobarbital binds at a distinct binding site associated with a Cl ⁻ ionopore at the GABA-A receptor, increasing the duration of time for which the Cl ⁻ ionopore is open ¹⁴ .	0.999
6	Gentisic acid		Shows a broad spectrum of biological activity, e.g. anti-inflammatory, antirheumatic, and antioxidant properties ¹⁴ .	Gentisic acid is also a byproduct of tyrosine and benzoate metabolism ¹⁴ .	0.999
7	Rose oxide		Show potential as anti-inflammatory with its ability to inhibit IL-1 β production ⁵³ .	Rose oxide is found in black elderberry and used as a flavoring agent ⁵³ .	0.999
8	Benzoyl acetone		Show potential as Retinoid acid receptor (RAR), retinoid X nuclear receptor alpha (RXR) inhibitor ³² .	Benzoyl acetone results in increased expression of CXCL8 mRNA ³² .	0.999
9	Aminoxaphen		Causes the characteristic effects of central nervous system stimulants like amphetamine and has been used clinically for its anorectic effects. Its adverse effects are also similar to those produced by central nervous system stimulants ¹⁴ .	Withdrawn from the market in 1968 in correspondence to significant incidence of pulmonary hypertension ¹⁴ .	0.999
10	Thymoquinone		Possess antiproliferative activity against a wide range of cancer cell lines i.e., Hela cells ³¹ .	Found in herbs and spices. Thymoquinone is a major constituent of seed oil of black cumin, <i>Nigella sativa</i> ³¹ .	0.999
11	Tocainide hydrochloride		Class I antiarrhythmic compound and useful in the treatment of ventricular arrhythmias ¹⁴ .	This drug decreases sodium and potassium conductance, thereby decreasing the excitability of myocardial cells ¹⁴ .	0.999
12	Cevimeline hydrochloride		Treatment for dry mouth associated with Sjögren's syndrome ¹⁴ .	Cevimeline binds and activate the muscarinic M1 and M3 receptors. The M1 receptors are generally found in secretory glands, and M3 receptors are found on smooth muscles and in many glands. The drug help to stimulate secretion in salivary glands, and thus relieve the symptom of dry mouth ¹⁴ .	0.999
13	Tigloidine		Tigloidine may provide relief in parkinsonian patients ⁵⁴ .	A type of Tigloyltropeine which is an alkaloid from <i>Physalis alkekengi</i> roots. In Parkinson treatment, the tigloidine works by increasing the gamma-efferent activity and reducing alpha motoneurone activity ⁵⁴ .	0.999
14	Finitin		-	A natural product found in Artemisia ³² .	0.999
15	Nupharamine		It has been used as a diuretic and for the treatment of stomachache ⁵⁵ .	Found in Japanese water lily, <i>Nuphar japonica</i> , found in Japan and Korea ⁵⁵ .	0.999
16	Diaboline		Diaboline is a glycine receptor antagonist and a convulsant ⁵⁶ .	A curare alkaloid obtained from the plant <i>Strychnos diabolii</i> ⁵⁶ .	0.999

^aAll drugs scored 0.99 when tested against the dengue NS3 protein and were ranked accordingly for further selection.

Table 4. List of Substances Screened and Filtered from the RF Model and Their Usage^a

#	Name	Chemical structure	Indication	Remarks	Score
1	Linalool		Established sedative, antidepressant, anxiolytic, and immune potentiating effects ⁵⁷ .	A noncyclic monoterpene, usually extracted from lavender (<i>Lavandula</i> spp.), rose (<i>Rosa</i> spp.), basil (<i>Ocimum basilicum</i>), and neroli oil (<i>Citrus aurantium</i>) ⁵⁷ .	0.730
2	Sesamine		Possess role as an antineoplastic agent, a neuroprotective agent and a plant metabolite ³² .	A natural product generally found in <i>Pandanus boninensis</i> , and <i>Podolepis rugata</i> ³² .	0.580

^aAll substances showed a score of ≥ 0.5 when tested against the dengue NS3 protein.

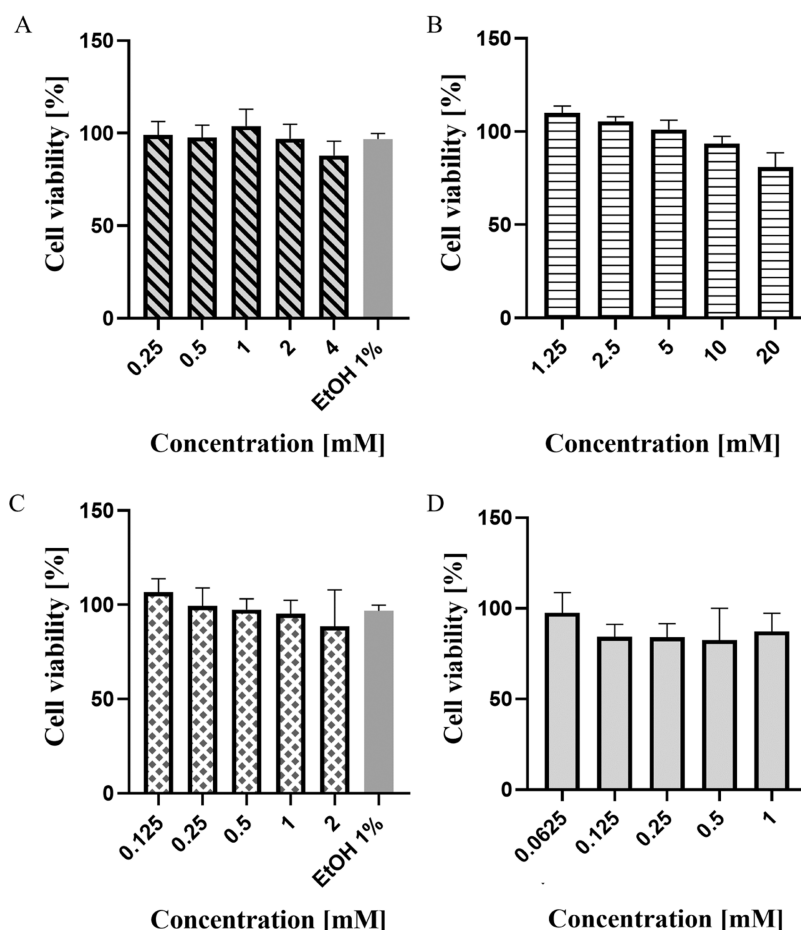


Figure 2. Viability of Vero cells after treatments with different drugs: (A) zileuton, (B) trimethadione, (C) linalool, and (D) positive control—ribavirin. The viability of cells was analyzed at 72 h using the MTT assay. No significant cell morphology changes were detected at the highest concentration tested. The CC_{50} values are expressed as percentages of treated *vs.* untreated cells. Each value is the means \pm SD of three experiments, each run in triplicate.

inhibitor that forms stable complexes and blocks the active sites of enzymes. At a concentration of 5 μ M, the protease inhibitor inhibited more than 65% of the protease activity and recorded the highest inhibition (>85%) at 10 μ M concentration. Another positive control, ribavirin, shows the opposite effect. The fluorescence intensifies with the addition of the treatment but gradually reduces the effect with the increase of drug concentration. This is an interesting outcome, as the effect on the NS2B-NS3 protease was inconsistent with the observed *in vitro* result. Thus, this finding suggests that the ribavirin does not work in targeting the NS2B-NS3 protease but inhibits the viral progression *via* different mechanisms. To

be specific, the mechanism of action of ribavirin is *via* lethal mutagenesis of RNA virus genomes mediated by the viral RNA-dependent RNA polymerase,¹⁶ and this may result in viral inhibition as reported in the study.

For zileuton, a positive correlation was observed between drug concentration and the percentage of inhibition. The highest protease inhibition (27.7%) was observed at a concentration of 4 mM, while at 2 mM concentration, the inhibition was reduced to 17.89%. For linalool, the drug recorded an average protease inhibition of 18.42% at 2 mM and 13.83% protease inhibition at 1 mM. For trimethadione, the highest protease inhibition (17.15%) was recorded at 20

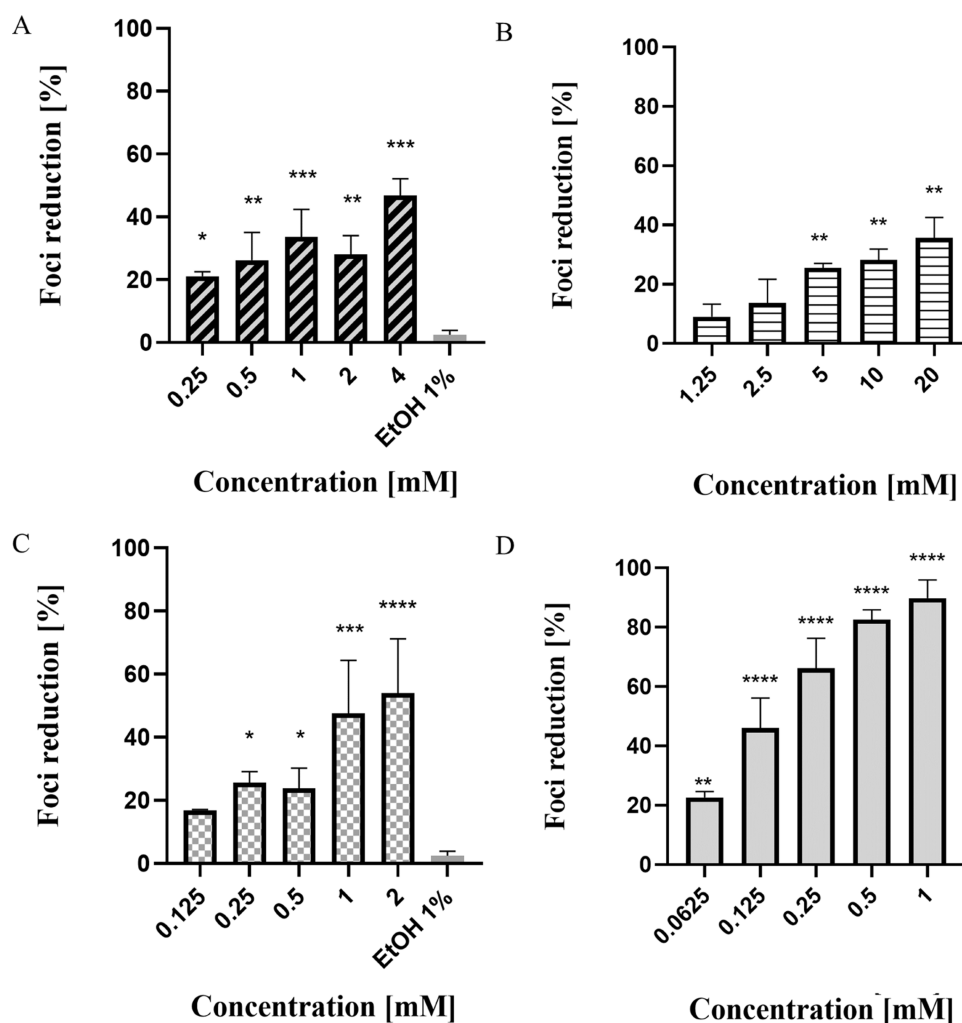


Figure 3. Inhibitory potential of drugs on infected cells with the dengue virus: (A) zileuton, (B) trimethadione, (C) linalool, and (D) positive control—ribavirin. The drug was diluted to various concentrations (as indicated above) with overlay media and added to the cell culture. The viral inhibition was analyzed at 72 h. The inhibitory response of each drug is expressed as the mean of absorbance \pm SD of three experiments, each run in triplicate. (* $p < 0.05$, ** $p < 0.01$, *** $p < 0.001$, **** $p < 0.0001$).

mM, and at 10 mM, about 13.17% of protease inhibition was detected. Overall, among all drugs, at the highest concentration tested, trimethadione showed the least effect on the protease activity (20 mM, 17.15% protease inhibition).

2.3. Development of New Compounds from the Combination of Selected Drugs. Based on the *in vitro* results, two new compounds were developed—ziltri and zilool (Figure 5). Zileuton was the main component for both ziltri and zilool, with ziltri—zileuton + trimethadione and zilool—zileuton + linalool. Zileuton was chosen to be the main component in the ziltri and zilool combination as it shows higher protease reduction.

2.4. Molecular Docking of the Selected Drugs and Newly Derived Compounds with the Dengue NS2B-NS3 Protease. The NS2B-NS3 protease is made up of 4 subpockets, S1-4 and the important residues include Asp129_NS3, Ser135_NS3, Tyr150_NS3, and Tyr161_NS3 (S1 pocket); Asp81_NS2B, Gly82_NS2B, Ser83_NS2B, Asp75_NS3, and Asn152_NS3 (S2); Ser85_NS2B, Ile86_NS2B, and Lys87_NS2B (S3); and Val154_NS3 and Ile155_NS3 (S4).²⁸ The docking site of the protease was determined from the halo form of the protease, which serves as the golden reference for the binding site. The site contains the

important catalytic triad of the protease, which are His51, Asp75, and Ser135. A mutagenesis study revealed that the replacement of catalytic serine with alanine caused the inactivity of the protease, and no viable virus was recovered from an infectious cDNA clone with abolished protease activity.^{17,18} The site is well known for its shallowness, and the prediction by the PockDrug¹⁹ server showed that this site has a druggability score of 0.5 (score range 0–1), which may reduce the ability of small molecules to effectively interact with the protein.

In the docking exercise, all drugs and the two newly developed compounds were found to bind to the binding pocket at the right side of the active site region (S1 pocket), as observed in Figure 6. Interestingly, this site is much broader and more shallow than the binding pocket at the left region (S2 pocket),²⁰ yet, most of the interactions were observed to be at this site. It was identified that the S1 region has much more hydrophobic residues compared to the S2 region. The summary of all interactions involved in the ligand–protein complexes is indicated in Figure 7 and Table 5.

From the molecular docking study, zileuton was shown to bind to the active site at -5.6 kcal/mol, as depicted in Figure 7A,B. From the result, zileuton formed 5 hydrogen bonds with

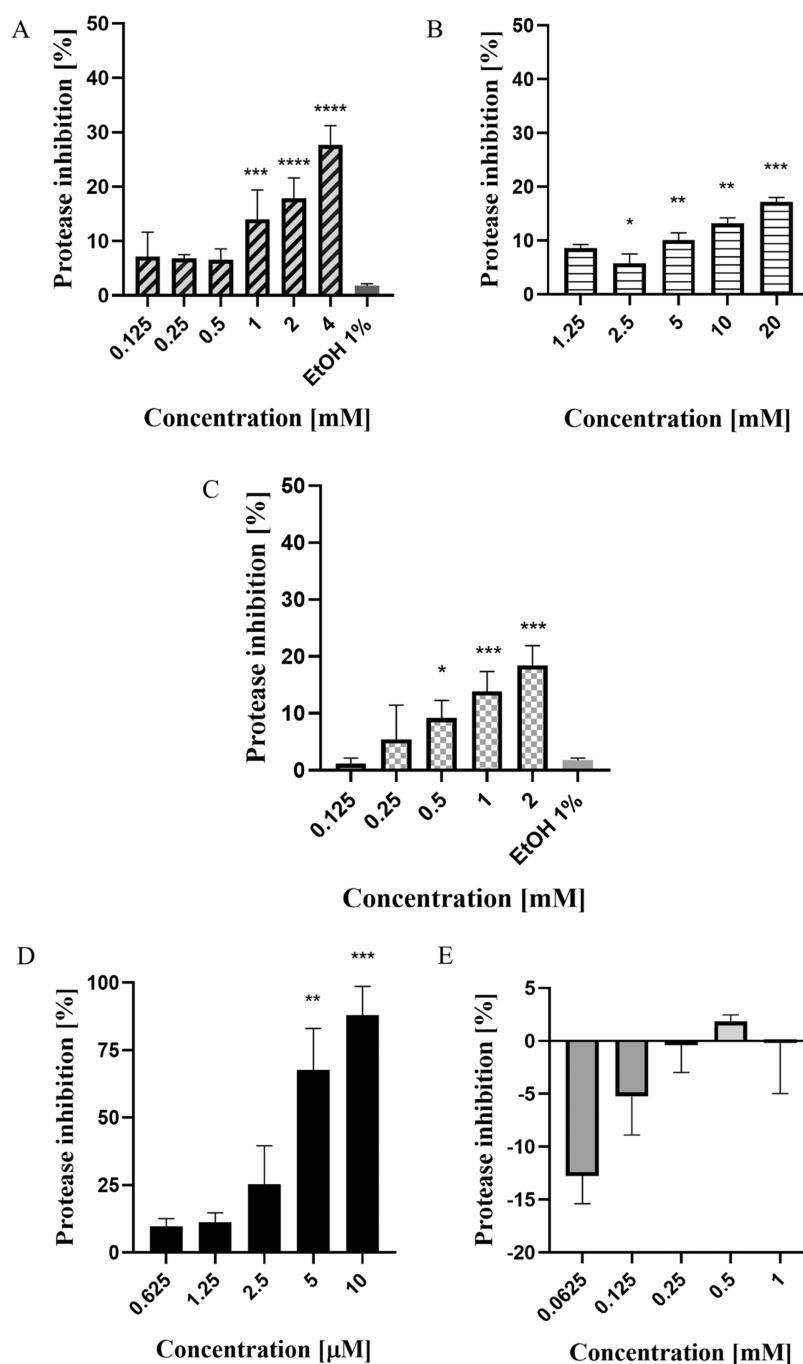


Figure 4. NS2B-NS3 protease inhibition with the treatment of selected drugs: (A) zileuton, (B) trimethadione, (C) linalool, (D) positive control, aprotinin, and (E) positive control—ribavirin. The statistical analysis was conducted between particular drugs against the untreated cells (NC) using one-way ANOVA with Tukey correction. Each value is the means \pm SD of two experiments, each run in triplicate. (* $p < 0.05$, ** $p < 0.01$, *** $p < 0.001$, **** $p < 0.0001$).

the NS2B-NS3 protease where one of the hydrogen bond interactions involved B:Ser135 of the catalytic triad at a distance of 3.4 Å. Other hydrogen bond interactions involved B:Phe130 (3.4 Å), B:Lys131 (3.2 Å), B:Gly133 (2.2 Å), and B:Tyr150 (3.5 Å), with either the amides or alcohol functional groups of zileuton. Moreover, zileuton formed alkyl interactions with B:Pro132 (3.8 Å) and van der Waals interactions with B:His51, B:Gly151, B:Asn152, and B:Tyr161.

The molecular docking of trimethadione is shown in Figure 7C,D. It was found that the drug also established a hydrogen bond with B:Ser135 at a distance of 2.5 Å. Other hydrogen

bond interactions were found between the drug–protein complex including B:Lys131 (3.2 Å), B:Thr134 (2.2 Å), and B:Gly133 (2.5 Å). Trimethadione also formed a σ - π bond with residue B:Tyr161 (3.7 and 3.9 Å) and an alkyl bond with B:Pro132 (4.9 Å). The van der Waals interaction occurs between trimethadione and residues B:Asp129, B:Lys131, B:Phe130, and B:Tyr150. The binding affinity for the complex above was predicted at -4.6 kcal/mol.

Linalool was found to form two polar interactions with the protease, as observed in Figure 7E,F. In addition to the interaction with B:Ser135, the hydroxyl group of linalool

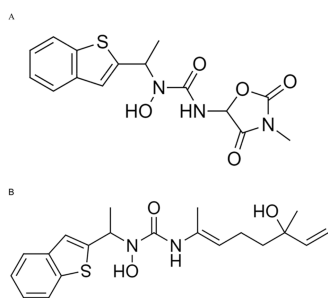


Figure 5. Newly developed compounds based on the *in vitro* results. (A) Ziltri (zileuton + trimethadione) and (B) zilool (zileuton + linalool).

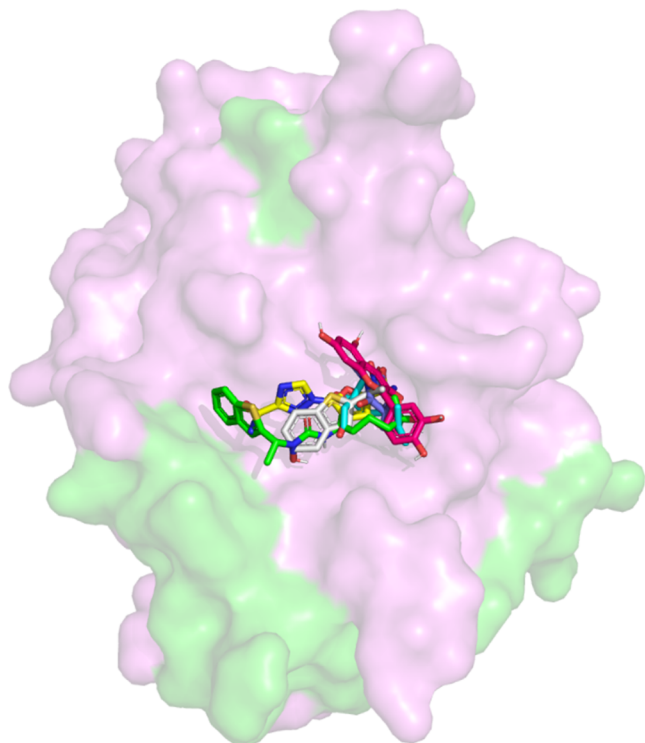


Figure 6. Molecular surface representation of the NS2B-NS3 protease with selected drugs. Selected drugs from two prediction models (zileuton, trimethadione, linalool), newly developed compounds (ziltri and zilool) and positive control—panduratin A, were docked at the active site of the protease.

established a hydrogen bond with B:His51 (3.3 Å), another residue of the catalytic triad. Besides His51, linalool also formed hydrogen bonding with B:Gly151 (2.3 Å). It was found that the drug formed σ - π and π -alkyl bonds with residue B:Tyr161. van der Waals forces were seen between linalool and residues B:His51, B:Asp129, B:Phe130, B:Gly133, and B:Tyr150. The predicted binding affinity for the complex was -4.1 kcal/mol.

In comparison to the selected drugs, the control, panduratin A, showed the highest binding affinity (-7.0 kcal/mol). The molecular docking study of panduratin A is shown in Figure 7K,L. It was observed that the panduratin A-protein complex established polar interactions with four amino acid residues, *i.e.*, B:Lys131 (3.4 Å), B:Gly133 (2.3 Å), B:Thr134 (2.3 Å), and B:Ser135 (2.4 Å). Besides, π - π T-shaped bonds were found between the ligand and B:His51 and B:Tyr161, while a π -alkyl bond was established with B:Pro132. Previously,

panduratin A showed competitive inhibition toward DENV-2 NS2B/NS3pro *in vitro* with $K_i = 25$ μ M,²¹ which shows the validity of this compound as the protease inhibitor and reference for the study.

Since the *in vitro* inhibitions of the selected drugs were found to be moderate, and the recorded binding affinities were less than panduratin A, we included two newly proposed compounds to be docked against the NS3 protease. These compounds were ziltri (Figure 7G,H) and zilool (Figure 7I,J). These combinations showed improved binding affinity as compared to the selected drugs. Ziltri showed the highest binding affinity (-7.7 kcal/mol), followed by zilool (-6.9 kcal/mol). Ziltri formed hydrogen bond interactions with B:Phe130 (2.8 Å), B:Tyr150 (1.9 Å), B:Gly151 (2.3 Å), B:Gly153 (2.2 Å), and B:Tyr161 (2.0 Å) and formed π -sulfur interactions with B:His51. It should be noted that both ziltri and zilool interact with at least one of the catalytic triad residues, with zilool also occupying the S2 pocket through an interaction with Asp75. In addition, both ziltri and zilool, as well as panduratin A, are larger in size compared to the three screened drugs. Hence, the larger ligand size may be another prerequisite when docking at shallow sites, as shown by the DENV-3 active site.

3. DISCUSSION

The aim of this study is to discover novel anti-dengue drugs from old drugs that target the DENV NS3 protein using a combination of *in silico* and *in vitro* studies. To achieve the desired objectives, three phases of the study were conducted. In the first phase, the screening of potential drugs was conducted by building a prediction model of established bioactivity data of the anti-dengue NS3 protein using two prediction models—L-B and PCM. Next, the process continued with the evaluation of the screened drugs' anti-dengue properties *in vitro* by using the FFURA assay and protease assay. The drugs were tested using similar concentrations throughout these three assays, and the effectiveness of viral inhibition was analyzed. Based on the observed *in vitro* results, molecular docking was conducted on the screened drugs and newly developed compounds against the DENV NS3 protein. The key binding interactions and the best binding orientation were determined.

Based on the results, several key observations can be deduced. **First, the L-B model performs slightly better than the pcm model in the prediction of anti-dengue potential.** In the external validation, the L-B model showed higher sensitivity compared to the PCM model (L-B = 0.671, PCM = 0.538). Meanwhile, the L-B model showed a lower sensitivity value in the internal validation; however, the difference is insignificant compared to the PCM model. In addition, external validation has more weightage compared to internal validation as it evaluates compounds or instances it has never seen before. Moreover, as the goal of the study is to screen active inhibitors against the dengue virus, we placed a higher weightage on models that has high sensitivity value. This is important as we would want to maximize the positive number of correct classifications. Hence, the result that we obtained from the L-B model fits the above criteria, and therefore it is better than the PCM model.

These results highlight that the additional protein descriptors employed in the PCM model may not be advantageous in this study. However, this result should not be generalized and should be observed on a case-to-case basis.

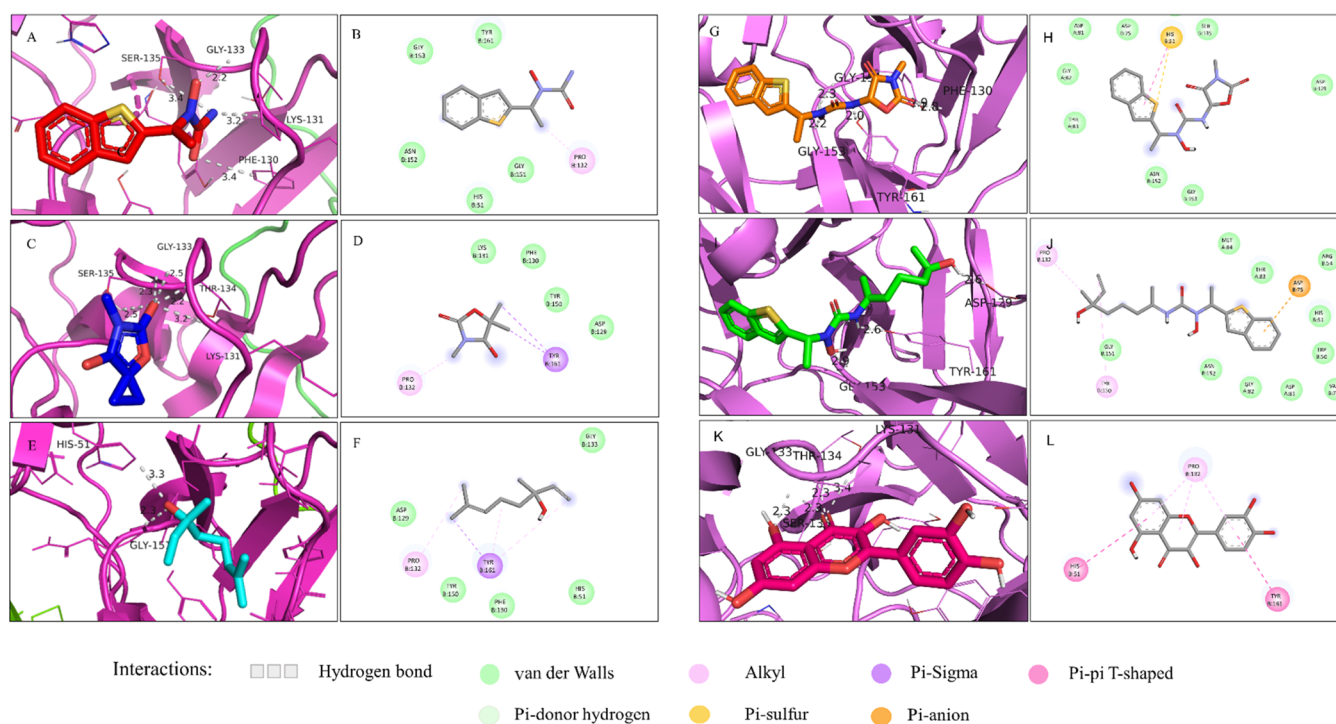


Figure 7. Interactions of the selected drugs and substances against the dengue NS2B-NS3 protease both in 3D and 2D visualizations. The complex of the NS2B-NS3 protease with zileuton (A, B), trimethadione (C, D), linalool (E, F), ziltri (G, H), zilool (I, J), and panduratin A (K, L).

Table 5. Affinity of the Different Complexes and the Residues Involved in the Interaction^a

drug	affinity (kcal/mol)	no. of H bonds	residue(s) involved in hydrogen bond interactions	residue(s) involved in other interactions
zileuton	-5.6	5	B:Phe130, B:Lys131, B:Thr134, B:Ser135, B:Tyr150	B:Pro132 (alkyl bond); B:His51, B:Gly151, B:Asn152, B:Tyr161 (van der Waals)
trimethadione	-4.6	4	B:Lys131, B:Gly133, B:Thr134, B:Ser135	B:Pro132 (alkyl bond); B:Thr161 (π - σ bond); B:Asp129, B:Lys131, B:Phe130, B:Tyr150 (van der Waals)
linalool	-4.1	3	B:His51, B:Ser135, B:Gly151	B:Tyr161 (alkyl, π - σ , and π -alkyl bonds); B:His51, B:Asp129, B:Phe130, B:Gly133 and B:Tyr150 (van der Waals)
ziltri (zileuton + trimethadione)	-7.7	5	B:Phe130, B:Tyr150, B:Gly151, B:Gly153, B:Tyr161	B:His51 (π -sulfur bond), A:Asp81, A:Gly82, A:Thr83, B:Asp75, B:Asp129, B:Ser135, B:Asn152, B:Gly153 (van der Waals)
zilool (zileuton + linalool)	-6.9	3	B:Asp129, B:Gly153, B:Tyr161	B:Asp75 (π -anion); B:Pro132, B:Tyr150 (alkyl and π -alkyl bonds); A:Asp81, A:Gly82, A:Thr83, A:Met84, B:Trp50, B:His51, B:Arg54, B:Val72, B:Gly151, B:Asn152 (van der Waals)
panduratin A	-7.0	4	B:Lys131, B:Gly133, B:Thr134, B:Ser135	B:His51, B:Tyr161 (π - π T-shaped); B:Pro132 (π -alkyl bond)

^aAll of the results were predicted using AMDock⁴⁹ software using Autodock Vina,⁵¹ while PyMOL⁴⁸ Open GL and Biovia Discovery Studio⁵² were used for visualization.

For example, a study by Lapins et al.²² demonstrated that the PCM model outperformed the QSAR model (that uses a single descriptor) for single target models to identify Cytochrome P450 (CYP) inhibition where the area under the curve was higher in PCM than QSAR (AUC:PCM > 0.90, QSAR 0.79–0.89). Further external validation of the PCM model showed an AUC score of 0.94, which suggested the good performance of the constructed PCM model. Nevertheless, the result presented by Lapins et al.²² uses a smaller number of proteins and compounds (5 CYPs and 17, 143 compounds) compared to the current study, which uses 10 proteins of different origins and more than 62,000 compounds, which may account for the disparity in results. In another study using a kinase data set spanning the whole kinome by Nijima et al.,²³ ligand-based models using SVMs performed better than PCM DC-SVMs in

external validation with an accuracy of 81.3% compared to 73.9%. Interestingly, for internal validation, the result presented by Nijima et al.²³ was comparable to the current study, where PCM dual component (DC)-SVMs showed higher accuracy compared to the L-B model, with 90.9% and 86.2%, respectively. The absence of the protein descriptors in the L-B model also resulted in a faster calculation and computational time compared to the PCM model. Despite these matters, both models have successfully screened drugs that were able to elicit moderate antiviral activities *in vitro* and biologically safe to the cell, although treatment was used at a high concentration. Hence, both methods can produce a comparatively fast and promising result to assist the anti-dengue NS3 drug development process.

Second, out of the three drugs that were screened, zileuton and linalool showed promising results *in vitro* as lead compounds for anti-DENV potential. This is based on the observed FFURA and protease assays. In the FFURA assay, linalool performed better than zileuton and trimethadione, while zileuton showed the highest inhibition of the DENV NS3 protease at the highest concentration tested, as well as in molecular docking. Therefore, both zileuton and linalool have the potential for further development of DENV NS3 protease inhibitors, as both consistently showed good efficacy in each assay. These drugs can be direct-acting antivirals (DAA) that specifically target the viral protein. Besides, these drugs show low toxicity even when tested at a high concentration, which fits the DAA criteria that includes drug efficacy at low toxicity and a wide treatment window. However, except for the protease assay, both drugs were unable to exhibit better results than ribavirin. In addition, the ability of linalool to inhibit the DENV NS3 protease and dengue-infected cells highlights another advantage of the L-B model. To increase our understanding of the chemical space of the active compounds against dengue, using PCA analysis, it was found that linalool was not located in the dense area as compared to trimethadione and zileuton (from PCM model), and yet, the activity from the *in vitro* validations showed promising antiviral results (see Supporting Information S1). Thus, this demonstrates the ability of the L-B model to predict compounds outside the chemical space covered by the training set. Although the drugs are no better than ribavirin in terms of foci inhibition, however, all of them showed better protease inhibition. This is true as ribavirin is not a specific inhibitor of the NS3 protease and is not currently used as a treatment for dengue fever. From the protease assay, we identified that ribavirin is not a suitable positive control for protease inhibition as it showed the opposite effect than inhibiting the protease, and therefore other positive controls such as aprotinin or panduratin A need to be used for this purpose.

One issue that may be raised from the study is the effective concentration used in the treatment. Unlike several studies that reported the success of inhibition at submicromolar concentration, the current study suggested the use of marketed drugs at a millimolar concentration to achieve a desirable antiviral effect. In exception to trimethadione, this issue may have arisen possibly due to the drugs' low solubility; however, there is not enough evidence to draw that poor bioavailability is the reason for this event. In one study investigating standard serine protease inhibitors against CF40.NS3pro, a recombinant NS3 protease, revealed that three out of 16 inhibitors only reduced the protease activity up to 15% at 1 mM concentration.²⁴ Therefore, this finding supports the results obtained from the current study, where some of the protease inhibitors may require high concentration to exhibit the desired property. In another study by Holbeck et al.²⁵ on the FDA-approved anticancer potential in the NCI60 human tumor cell lines, at least three drugs exhibit 50% growth inhibition (GI_{50}) at the concentration of $\geq 2500 \mu\text{mol/L}$ (2.5 mM). This inferred that some drugs do exhibit their activity at higher concentrations when tested *in vitro* while still remaining safe and effective to be used in patients for anticancer treatment.

Third, interactions with the residues of the catalytic triad, ligand size, and binding at S1 and S2 subpockets may be important prerequisites in establishing strong binding against ns3 proteins at the active site. From the results, we hypothesized that the interaction of the selected drugs and

proposed compounds with one of the catalytic triad residues, *i.e.*, Ser135 of the NS3 protease, might disrupt the electron exchange between the carboxyl group of Asp75 and the nitrogen atom of the imidazole ring of His51.²⁶ This may disturb the capability of His51 to trigger nucleophilic assault of the hydroxyl group ($\beta\text{-OH}$) of Ser135, which is important for the initiation of proteolysis.^{26,27} In addition, all ligands were found to have interactions with one or more amino acid residues (Asp129, Phe130, Tyr150, Asn152, and Gly153) of NS3 protease pocket 1 and its vicinity. Apart from that, these residues form a small part of the β -sheet that has an important role in substrate binding.^{1,2} Hence, such interactions possibly alter the functional attribute of the protein by changing its conformation.

In addition to the previous point, hydrogen bonding may be important for a stable interaction against the catalytic triad and other important residues of NS3. When comparing the docking results of the screened drugs, the more the hydrogen bonds established with NS3, the lower the binding energy. Our finding is in line with Hariono et al.,²⁸ where hydrogen bonds are responsible for the stability of the thioguanine scaffold derivative-protease complex. Compound 18, the best derivative of the scaffold with the lowest IC_{50} value (0.38 μM), formed 26 hydrogen bonds, which have at least 0.1% occupancy throughout 70 ns simulation time. A hydrophobic interaction, to a lesser extent, was also observed to maintain the stability of the complex. Furthermore, Katz et al.²⁹ identified a serine protease inhibition motif in which binding is mediated by a cluster of very short hydrogen bonds ($< 2.3 \text{ \AA}$) at the active site between the protein residues and the inhibitor. However, when comparing the screened drugs and newly proposed drugs, although the latter formed lesser hydrogen bonds, its binding energy was lower. In addition, all compounds occupy both subpockets 1 and 2 (S1 and S2), and in shallow and broad binding pockets such as S1, the size of the compounds plays an important role. It has been reported that shallow pockets are not "druggable sites" where it is difficult for small-sized compounds to be flanked by the binding pocket. In addition, the estimated K_i for ziltri was 2.69 μM , which is smaller than the estimated value of panduratin A, which is 7.4 μM , which makes it a better inhibitor than the reference drug. Based on these observations, we anticipated that ziltri and zilool may show better *in vitro* viral inhibition as the results showed higher binding affinity than the positive control, panduratin A.

4. CONCLUSIONS

This study attempted to repurpose old drugs as novel DENV NS3 inhibitors using *in silico* screening and validation of the antiviral properties of selected drugs *via in vitro* assays and molecular docking. Based on the results, three key findings can be deduced, which are: (i) the L-B model slightly outperforms the PCM model in DENV NS3 screening, (ii) zileuton and linalool showed promising results, and (iii) besides the interaction with the catalytic triad, the size of the compounds may be another important prerequisite, given the shallowness of the binding site. In regards to (iii), this observation was made when two newly proposed compounds, ziltri (zileuton + trimethadione) and zilool (zileuton + linalool), were docked to NS2B-NS3 and showed the overall lowest binding energy surpassing the positive control, panduratin A. These compounds were proposed to produce compounds with better viral inhibition. This is because the individual drugs showed inhibition in the millimolar concentration, although some

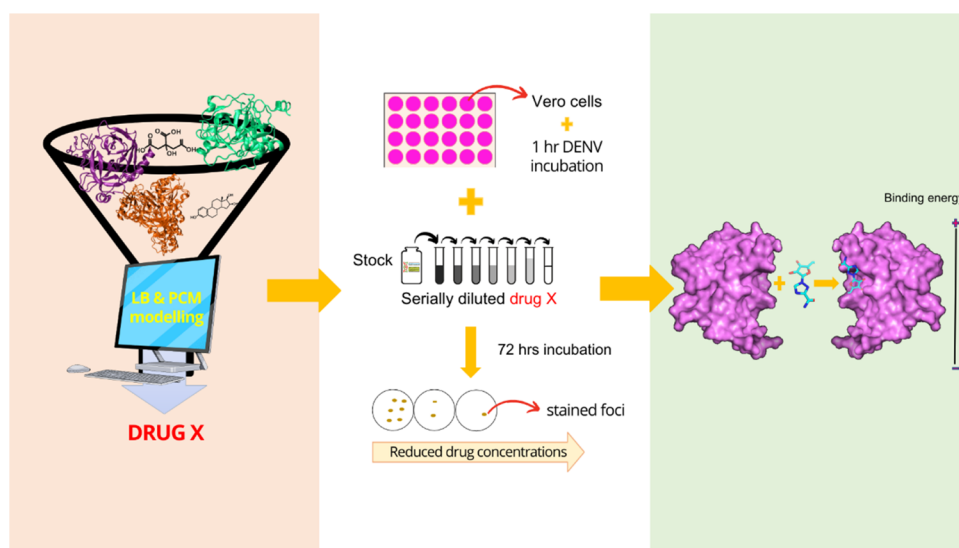


Figure 8. Workflow of the study. The study begins with building a prediction model that could screen marketed drugs for activity against the NS3 dengue protein. Here, ligand-based (LB) and proteochemometric (PCM) models were developed. Next, the *in vitro* validations were conducted to analyze the antiviral properties of the drugs. Here, the cytotoxicity assay, FFURA, and protease inhibition assay were conducted. The final stage of the evaluation was done to determine factors that possibly contribute to the interaction observed *in vitro* using molecular docking. Here, molecular docking was done on the selected drugs against the NS3 protease. The binding energy and the interactions that developed between the ligand–protein complexes were analyzed.

drugs do exhibit *in vitro* activity at such concentrations.³⁰ It should be noted that all compounds contain several stereocenters, which may complicate their synthesis. Future studies should include more bioactivity data from the viral serine protease, which, at the time of the study, was limited, and the size of the ligands should be considered in the screening. In addition, drug filtering parameters prior to the prediction process may need to be reconsidered the chemical features of the ligand, which could fit the shallow and broad active site of the NS3 protease. Furthermore, molecular dynamics should be performed as it provides better insights into the ligand–protein interaction in a fixed period of time, giving a view of the dynamic “evolution” of the system. At this juncture, the three screened drugs (zileuton, linalool, and trimethadione) are much more suitable to be considered as lead compounds for DENV NS3, and hence, this study has provided five new lead compounds for NS3 that can be further modified to improve their activity.

5. MATERIALS AND METHODS

5.1. *In Silico* Target Prediction. The study was conducted in several phases, as illustrated in Figure 8. Initially, the screening of the anti-dengue potential was conducted using *in silico* target prediction. Here, the target prediction was employed using machine learning to predict the most probable protein targets of small molecules. The algorithms that were employed in machine learning use protein sequence data to learn patterns and uncover relationships between target proteins and the possible biological activities of the compounds/substances using carefully prepared chemical libraries. In short, the predictions are based on the similarity principle through reverse screening.

5.1.1. Training Set. To build a predictive model, 62,746 active and inactive compounds related to 10 proteins associated with, and including, the NS3 protein were retrieved from ChEMBL,³¹ PubChem,³² and BindingDB³³ databases, as indicated in Table 6. Three of the NS3 proteins belong to the

Table 6. Breakdown of Bioactivity Data Points Collected for Each Targeted UniProt ID^a

protein	uniprot ID	active	inactive	total
dengue virus genome polyprotein	P14337	6271	29,929	36,200
hepatitis C virus genome polyprotein	P26662	2680	7643	10,323
West Nile virus genome polyprotein	P06935	137	617	754
prothrombin	P00734	3274	728	4002
coagulation factor X	P00742	5204	358	5562
serine protease 1	P07477	1930	204	2134
neutrophil elastase	P08246	2154	257	2411
cathepsin G	P08311	231	57	288
kallikrein-7	P49862	46	26	72
coagulation factor IX	P00740	593	15	608
	total	22,520	39,834	62,354

^aBioactivity data were collected from PubChem,³² ChEMBL,³¹ and BindingDB.³³

Flaviviridae family, which are the dengue virus (DENV), West Nile virus (WNV), and Hepatitis C virus (HCV) (UniProt ID P14337, P06935, P26662, respectively). Since NS3 is a serine protease, therefore we incorporated another seven human serine proteases into the training set as bioactivity data on viral serine protease is limited. An active ligand–protein interaction was considered as having a $K_i/K_d/IC_{50}$ /percentage inhibition value of less than 50 μ M or 50%. Any values above the specified threshold were considered as inactive. All protein sequences were collected from UniProt.³⁴

5.1.2. Chemical Descriptor. To represent the compounds as vectors for both PCM and L-B models, the Extended Connectivity Fingerprints with a diameter of four bonds (ECFP₄)³⁵ and a bit size of 1,024 was used as a chemical fingerprint as this fingerprint has proved to effectively secure

the chemical structural information relevant to bioactivity in several studies.^{35,36}

5.1.3. Machine Learning Algorithms for the PCM Model.

For the PCM model, the protein vectors were represented by their full sequence, where a protein sequence is denoted as a string of characters, and each character represents an amino acid that is part of the protein. The Parzen Rosenblatt Windows (PRW)^{37,38} was employed as a classification algorithm, and based on the Bayes theorem, compound x was assigned to class ω_α with the highest value. The posterior probability, or probability of a new compound belonging to a target class, ω_ω with a given vector molecular feature, \mathcal{H} , is calculated as such

$$p(\omega_\alpha|\mathcal{H}) = \frac{p(\mathcal{H}|\omega_\alpha) \cdot p(\omega_\alpha)}{p(\mathcal{H})} \quad (1)$$

$$\text{posterior probability} = \frac{\text{likelihood} \cdot \text{prior probability}}{\text{evidence}}$$

The *a priori* probability of class ω_α , $P(\omega_\alpha)$, can be calculated as the class proportion in the training set. The quantity $p(x|\omega_m)$ is the class conditional probability of x belonging to class ω_m and $p(x)$ is the normalization constant, which assures that the sum of all of the M class conditional probabilities is equal to one and is hence given by

$$p(x) = \sum_{m=1}^M p(\omega_m)p(x|\omega_m) \quad (2)$$

The PRW calculates the class conditional probability $p(x|\omega_\alpha)$ as the average similarity of the unknown compound, x , against a set of known compounds, x_j , belonging to a given class ω_α . The value $p(x|\omega_\alpha)$ is given by

$$p(x|\omega_\alpha) = \frac{1}{N_{\omega_\alpha}} \sum K(x, x_j; \lambda) \quad (3)$$

The equation above then becomes as below once we incorporate biological similarity using the tensor product shown before

$$p(x, t|\omega_\alpha) = \frac{1}{N_{\omega_\alpha}} \sum_{(x_j, t_j) \in N_{\omega_\alpha}} K(x, x_j; \lambda) \otimes K(t, t_j) \quad (4)$$

Here, (x, t) is the compound–target complex being analyzed and N_{ω_α} and (x_j, t_j) are the number of compound–target pairs and compound–target pairs in class ω_α , respectively.

5.1.3.1. Chemical Similarity Measurement. As the component of the PCM model, the Aitchison–Aitken (AA) kernel³⁹ was used to calculate chemical similarity.

$$K(x, x_j) = \lambda^{n-d} (1 - \lambda)^d \quad (5)$$

$$= e^{\log \lambda^{n-d}} \cdot e^{\log(1-\lambda)^d} \quad (6)$$

$$= e^{(n-d)\log \lambda} \cdot e^{d\log(1-\lambda)} \quad (7)$$

$$= e^{n\log \lambda} \cdot e^{-d\log(\lambda/1-\lambda)} \quad (8) \quad (5)$$

where $d = (x - x_j)^T(x - x_j)$ means the number of times x and x_j differ, λ is the smoothing parameter, and n is the size of the compound vector, which, in this case, is 1024. The smoothing parameter in the AA kernel has a narrow range of $0.5 < \lambda < 1.0$. At $\lambda = 0.5$, it will produce maximum smoothing, and at $\lambda = 1.0$,

no smoothing occurs; hence, these two values are ignored.³⁹ For this study, the AA kernel was executed at $\lambda = (0.8, 0.83, 0.86, 0.89, 0.9, 0.93, 0.96, 0.99)$.

5.1.3.2. Biological Similarity Measurement. The protein sequences were subjected to sequence alignment using multiple sequence alignment named MUSCLE⁴⁰ on the EMBL-EBI server (<https://www.ebi.ac.uk/Tools/msa/muscle/>). The protein sequence similarity is calculated as the ratio of the number of matching amino acids over the length of alignment using the package bio3d in R.⁴¹ Sequence alignments are performed to identify the structural, functional, or evolutionary relationships that may exist between protein sequences by aligning the sequences to find regions of similarity.

5.1.4. Machine Learning Algorithms for the L-B Model. A random forest (RF) algorithm was used to build the L-B prediction model. There are two stages in producing the RF algorithm: RF creation and prediction. In RF creation, k features are randomly selected from total m features where $k \ll m$. Among the k features, node d is calculated using the best split point, using the Gini index (S).

$$\text{Gini}(S) = 1 - \sum_1^j P(i) \quad (9)$$

The node is then split into daughter nodes using the best split. All of the steps were repeated until i number of nodes had been reached. j is the number of class and $P(i)$ is the probability of an instance being classified to a specific class. The node is then split into daughter nodes using the best split. All the steps were repeated until i number of nodes had been reached.

This process will repeat until the tree has reached the specified number of branches; nodes were expanded, and a path was established. As RF is an ensemble of decision trees, the number of trees, n was set at 100. In the next stage, which is the random forest prediction, test features are taken and rules of each randomly created decision tree to predict the outcome is used and predicted outcome is stored. The average score from each tree is used as the final prediction from the RF algorithm.

5.1.5. Internal and External Validations. The internal validation was performed using 5-fold cross-validation. In brief, the data set was split into five subsets, where four were used as the training set, and the fifth served as the test set to assess the predictive ability of the model. In the first iteration, the first fold is used to test the model, and the rest are used to train the model. This process is repeated until each fold of the 5-fold has been used as the testing set. The external validation was performed by testing 18,820 compounds collected from the ZINC database (<https://zinc.docking.org/>), which are not in the training set.

5.1.6. Performance Measure. The model performance was measured using sensitivity and specificity metrics. This was calculated by the number of true positive (TP), true negative (TN), false positive (FP), and false negative (FN) compounds, as indicated below

$$\text{sensitivity} = \frac{\text{TP}}{\text{TP} + \text{FN}} \quad (10)$$

$$\text{specificity} = \frac{\text{TN}}{\text{TN} + \text{FP}} \quad (11)$$

5.1.7. Applicability Domain (AD) Using Cosine (\cos_θ) and Leverage. The cosine similarity is used to measure the similarity of the datasets regardless of the magnitude of the vectors. It measures the angle between two vectors starting at the origin and extending to the a -th and b -th p -dimensional objects.⁴² The cosine value ranges between 0 and 1, where a value of 1 indicates perfect similarity. Leverage is the other method that was applied to define the AD, where it uses the approach of extent of extrapolation. Both cosine and leverage were analyzed using similarity search nodes and leverage nodes,^{43,44} respectively, from the Knime⁴⁵ Analytics Platform. For leverages, compounds with a score ≥ 0.5 were considered reliable, while a score lower than the said value was considered unreliable. For similarity search, the output was directly determined as reliable and unreliable.

5.1.8. Drug Selection for In Vitro Validation Studies. 4548 drugs from the ATC classification J: anti-infectives for systemic use from the DrugBank¹⁵ and SWEETLEAD¹⁴ (structures of well-curated extracts, existing therapies, and legally regulated entities for accelerated discovery) databases were collected for dengue antiviral screening. The SWEETLEAD¹⁴ database included approved drugs, chemical isolates from traditional medicinal herbs, and regulated chemicals. Initially, the drug data set was screened to remove any redundancy with the data in the training set. Next, additional screening was conducted to the data set based on the corresponding physicochemical properties, *i.e.*, the hydrogen bond acceptor (≤ 6), hydrogen bond donor (≤ 2), rotatable bond count (≤ 10), Lipinski rule of five ($=0$), total polar surface area (≤ 100), and molecular weight (< 500 Da). These criteria were selected based on the average (mean) value of each property listed above from the pool of collected active drugs. In total, 1263 drugs were tested against the prediction models, and the cutoff value is set at ≥ 0.5 for both PCM and L-B models. Due to the large number of drugs from the PCM model that scored ≥ 0.5 , only drugs that scored 0.99 were considered for further *in vitro* analysis.

5.2. In Vitro Evaluation of Selected Drugs for the Anti-Dengue Potential. **5.2.1. Preparation of the Compounds.** The stock solutions of selected anti-dengue drugs, which are zileuton (Sigma-Aldrich, USA) and linalool (Santa Cruz Biotechnology, USA), were dissolved in ethyl alcohol (EtOH) (Sigma-Aldrich, USA), while trimethadione (Sigma-Aldrich, USA) and ribavirin (Sigma-Aldrich, USA) were dissolved in distilled water. The stock solution was filter-sterilized (0.22 μm pore, Bioflow, Malaysia) and further diluted with culture medium to the desired concentration for the assays.

5.2.2. Determination of the Drug Cytotoxicity Dose. The cytotoxicity assay was performed on the Vero cells. The cytotoxicity assay was carried out by seeding 1.5×10^4 cells into 96-well flat-bottom plates (Corning, USA). The plates were incubated in a 5% CO_2 humidified incubator for 24 h. Next, the cells were treated with a serially diluted stock of the test anti-dengue drugs at different concentrations and further incubated at 37 °C with 5% CO_2 . After 72 h, 10 μL of 3-(4,5-dimethylthiazol-2-yl)2,5-diphenyltetrazolium bromide (MTT) (Nacalai Tesque, Japan) (5 mg/mL) solution was added and incubated for 4 h. After incubation, the solution was carefully removed, and 100 μL of DMSO (Sigma-Aldrich, USA) was added, followed by continuous shaking for 10 min. The absorbance was measured using a microplate reader (Tecan, Austria) at 570 nm. The percentage of cell viability was determined based on the absorbance readings. The 50%

cytotoxic concentration (CC_{50}) value was calculated using GraphPad Prism 8.0.1 (GraphPad Software, Inc., San Diego, CA).

5.2.3. Determination of Viral Inhibition via the Foci Forming Unit Reduction Assay (FFURA). The antiviral activity of NS3 inhibitors was determined and evaluated by measuring the reduction in the number of DENV infectious foci after treatment. Briefly, 200 μL of DENV-2 (MOI of 1) was introduced to Vero cells and incubated for an hour. Later, the viral mixtures were removed, and cells were washed with phosphate-buffered saline (PBS). Prior to this, drug treatment at different concentrations was prepared using 2% fetal bovine serum (FBS) and 1.5% carboxymethyl cellulose (CMC) as the incubation medium. The cells were incubated with treatment media for three days. Virus foci were visualized according to the previously described method.⁴⁶ One foci is recognized as a clump of cells stained as light brown under the microscope, whereas under the naked eye, the foci appeared as brown spots. The number of foci was counted and recorded in duplicates, and the average was taken into account. The experiment was repeated three times. Half-maximal inhibitory concentrations (IC_{50}) were obtained through the dose–response curve analysis using GraphPad Prism 8.0.1. (GraphPad Software, Inc., San Diego, CA). The results were expressed as the mean values \pm standard deviation (SD) (the corresponding error bars were displayed in the graphical plots).

5.2.4. DENV NS2B-NS3pro Inhibition Assay. The protocol that was used for this assay was based on the study by Rothan *et al.*⁴⁷ In brief, reaction mixtures of 100 μL were prepared, which consisted of a 20 μM fluorogenic peptide substrate (Boc-Gly-Arg-Arg-AMC), 2 μM recombinant NS2B-NS3pro, and tested drugs at different concentrations. A Tecan Infinite M200 Pro fluorescence spectrophotometer was used to measure the absorbance with emission at 440 nm upon excitation at 360 nm. The intensity measurement was carried out after 30 min of incubation, and the results were expressed as a percentage of the negative control (noninhibitor compound, only substrate, enzyme, and buffer), which was always taken as 100%. All experiments were performed in triplicate and repeated three times. The results were expressed as the mean values \pm SD (the corresponding error bars were displayed in the graphical plots).

5.3. Molecular Docking of the NS3 Protease against the Selected Substances. The interaction between the selected drugs and DENV NS2B-NS3pro was identified by the molecular docking study. Here, the template of DENV-3 NS2B-NS3pro was used (PDB: 3U1I) for all docking activities as it showed 89% sequence similarities with DENV-2 NS2B-NS3pro. For docking, only chains A and B from protein PDB 3U1I were used as the template, while other chains and co-crystallized ligands were removed. In addition, water molecules and heterogroups were deleted from the structure by using PyMOL⁴⁸ software. The protein was prepared directly in AMDock⁴⁹ software, where protonation was performed using integrated PDB2PQR⁵⁰ that utilized the Amber forcefield at pH 7.4. Based on the *in vitro* result, panduratin A was included as the reference drug for the docking study. Zileuton and trimethadione structures were obtained from the DrugBank¹⁵ database in a PDB format, while linalool and panduratin A were retrieved from the PubChem³² database in the SDF format. The structures for compounds ziltri (combination of zileuton and trimethadione) and zilool (combination of zileuton and linalool) were drawn using Chemspace (Chem-

space.com/home), and the SMILES code was obtained from a similar source. All SMILES and SDF formats were converted to PDB using the Online SMILES Translator and Structure File Generator (<https://cactus.nci.nih.gov/translate/>). The grid box size and the grid spacing were set around the catalytic triad to a $20 \times 20 \times 20$ dimension and 0.375 Å, respectively, with the center set at $x = 21.1$, $y = -16.0$, and $z = 8.1$ using AutoDockTools (ADT). Docking simulations were performed using AMDock⁴⁹ using AutoDock Vina.⁵¹ AutoDock Vina⁵¹ generates different ligand conformers using a Broyden–Fletcher–Goldfarb–Shanno (BFGS) algorithm. The BFGS algorithm is implemented with an iterated local method search. Final docking output files were analyzed for hydrogen bonds and other interactions using integrated PyMOL⁴⁸ software in AMDock⁴⁹ and Discovery Studio Visualizer.⁵²

■ ASSOCIATED CONTENT

SI Supporting Information

The Supporting Information is available free of charge at <https://pubs.acs.org/doi/10.1021/acsomega.3c02607>.

Additional details from principal component analysis (PCA) of the chemical space of the prediction models, percentage of the variance of the top 10 PCs, and eigenvalue of the training set (PDF)

■ AUTHOR INFORMATION

Corresponding Author

Fazlin Mohd Fauzi – Department of Pharmacology and Pharmaceutical Chemistry, Faculty of Pharmacy, UiTM Selangor, 42300 Bandar Puncak Alam, Selangor, Malaysia; Collaborative Drug Discovery Research, Faculty of Pharmacy, Universiti Teknologi MARA Selangor, 42300 Bandar Puncak Alam, Selangor, Malaysia; orcid.org/0000-0002-1572-9449; Email: fazlin5465@uitm.edu.my

Authors

Zafirah Liyana Abdullah – Department of Pharmaceutical Life Sciences, Faculty of Pharmacy, Universiti Teknologi MARA Selangor, 42300 Bandar Puncak Alam, Selangor, Malaysia

Hui-Yee Chee – Department of Medical Microbiology, Faculty of Medicine and Health Sciences, Universiti Putra Malaysia, 43400 UPM Serdang, Selangor, Malaysia

Rohana Yusof – Department of Molecular Medicine, Faculty of Medicine, University of Malaya, 50603 Kuala Lumpur, Malaysia

Complete contact information is available at: <https://pubs.acs.org/doi/10.1021/acsomega.3c02607>

Author Contributions

Z.L.A.—conceptualization, data analysis, and writing—review & editing; H.-Y.C.—writing—review & editing; R.Y.—writing—review & editing; and F.M.F.—conceptualization, data analysis, and writing—review and editing.

Notes

The authors declare no competing financial interest.

■ ACKNOWLEDGMENTS

This research was supported by the Ministry of Education, Malaysia, through the Fundamental Research Grant Scheme (FRGS/1/2016/SKK10/UITM/02/1).

■ REFERENCES

- (1) World Health Organization. Dengue and Severe Dengue, 2018. <http://www.who.int/news-room/fact-sheets/detail/dengue-and-severe-dengue>. (accessed October 26, 2018).
- (2) Dengue Worldwide Overview, 2022. <https://www.ecdc.europa.eu/en/dengue-monthly>. (accessed July 06, 2022).
- (3) Obi, J. O.; Gutiérrez-Barbosa, H.; Chua, J. V.; Deredge, D. J. Current Trends and Limitations in Dengue Antiviral Research. *Trop. Med. Infect. Dis.* **2021**, *6*, No. 180.
- (4) First FDA-approved vaccine for the prevention of dengue disease in endemic regions [Press release] U.S. Food and Drug Administration. <https://www.fda.gov/news-events/press-announcements/first-fda-approved-vaccine-prevention-dengue-disease-endemic-regions> (accessed July 27, 2023).
- (5) Low, J. G. H.; Ooi, E. E.; Vasudevan, S. G. Current Status of Dengue Therapeutics Research and Development. *J. Infect. Dis.* **2017**, *215*, S96–S102.
- (6) Gu, F.; Shi, P.-Y. The Challenges of Dengue Drug Discovery and Development. *Clin. Invest.* **2014**, *4*, 683–685.
- (7) Behnam, M. A. M.; Nitsche, C.; Boldescu, V.; Klein, C. D. The Medicinal Chemistry of Dengue Virus. *J. Med. Chem.* **2016**, *59*, 5622–5649.
- (8) de Oliveira, A. S.; da Silva, M. L.; Oliveira, A. F. C. S.; da Silva, C. C.; Teixeira, R. R.; De Paula, S. O. NS3 and NSS Proteins: Important Targets for Anti-Dengue Drug Design. *Braz. Chem. Soc.* **2014**, *25*, 1759–1769.
- (9) Tomlinson, S. M.; Malmstrom, R. D.; Russo, A.; Mueller, N.; Pang, Y.-P.; Watowich, S. J. Structure-Based Discovery of Dengue Virus Protease Inhibitors. *Antiviral Res.* **2009**, *82*, 110–114.
- (10) Lin, K.-H.; Nalivaika, E. A.; Prachanronarong, K. L.; Yilmaz, N. K.; Schiffer, C. A. Dengue Protease Substrate Recognition: Binding of the Prime Side. *ACS Infect. Dis.* **2016**, *2*, 734–743.
- (11) Rahman, M. M.; Biswas, S.; Islam, K. J.; Paul, A. S.; Mahato, S. K.; Ali, M. A.; Halim, M. A. Antiviral Phytochemicals as Potent Inhibitors against NS3 Protease of Dengue Virus. *Comput. Biol. Med.* **2021**, *134*, No. 104492.
- (12) Bakulin, I.; Pasechnikov, V.; Varlamicheva, A.; Sannikova, I. NS3 Protease Inhibitors for Treatment of Chronic Hepatitis C: Efficacy and Safety. *World J. Hepatol.* **2014**, *6*, 326–339.
- (13) Liu, Z.; Fang, H.; Reagan, K.; Xu, X.; Mendrick, D. L.; Slikker, W.; Tong, W. In Silico Drug Repositioning – What We Need to Know. *Drug Discovery Today* **2013**, *18*, 110–115.
- (14) Novick, P. A.; Ortiz, O. F.; Poelman, J.; Abdulhay, A. Y.; Pande, V. S. SWEETLEAD: An in Silico Database of Approved Drugs, Regulated Chemicals, and Herbal Isolates for Computer-Aided Drug Discovery. *PLoS One* **2013**, *8* (11), No. e79568.
- (15) Wishart, D. S.; Feunang, Y. D.; Guo, A. C.; Lo, E. J.; Marcu, A.; Grant, J. R.; Sajed, T.; Johnson, D.; Li, C.; Sayeeda, Z.; Assempour, N.; Iynkkaran, I.; Liu, Y.; Maciejewski, A.; Gale, N.; Wilson, A.; Chin, L.; Cummings, R.; Le, D.; Pon, A.; Knox, C.; Wilson, M. DrugBank 5.0: A Major Update to the DrugBank Database for 2018. *Nucleic Acids Res.* **2018**, *46*, D1074–D1082.
- (16) Huchting, J. Targeting Viral Genome Synthesis as Broad-Spectrum Approach against RNA Virus Infections. *Antiviral Chem. Chemother.* **2020**, *28*, No. 204020662097678.
- (17) Katzenmeier, G. Inhibition of the NS2B–NS3 protease: towards a causative therapy for dengue virus diseases. *Dengue Bull.* **2004**, *28*, 58–67.
- (18) Valle, R. P. C.; Falgout, B. Mutagenesis of the NS3 Protease of Dengue Virus Type 2. *J. Virol.* **1998**, *72*, 624–632.
- (19) Hussein, H. A.; Borrel, A.; Geneix, C.; Petitjean, M.; Regad, L.; Camproux, A.-C. PockDrug-Server: A New Web Server for Predicting Pocket Druggability on Holo and Apo Proteins. *Nucleic Acids Res.* **2015**, *43*, W436–W442.
- (20) Othman, R.; Othman, R.; Baharuddin, A.; Ramakrishnan, N. R.; Abd Rahman, N.; Yusof, R.; Karsani, S. A. Molecular Docking Studies of Selected Medicinal Drugs as Dengue Virus-2 Protease Inhibitors. *Sains Malays.* **2017**, *46*, 1865–1875.

- (21) Kiat, T. S.; Pippen, R.; Yusof, R.; Ibrahim, H.; Khalid, N.; Rahman, N. A. Inhibitory Activity of Cyclohexenyl Chalcone Derivatives and Flavonoids of Fingerroot, *Boesenbergia Rotunda* (L.), towards Dengue-2 Virus NS3 Protease. *Bioorg. Med. Chem. Lett.* **2006**, *16*, 3337–3340.
- (22) Lapins, M.; Worachartcheewan, A.; Spjuth, O.; Georgiev, V.; Prachayasittikul, V.; Nantasenamat, C.; Wikberg, J. E. S. A Unified Proteochemometric Model for Prediction of Inhibition of Cytochrome P450 Isoforms. *PLoS One* **2013**, *8*, No. e66566.
- (23) Nijima, S.; Shiraiishi, A.; Okuno, Y. Dissecting Kinase Profiling Data to Predict Activity and Understand Cross-Reactivity of Kinase Inhibitors. *J. Chem. Inf. Model.* **2012**, *52*, 901–912.
- (24) Leung, D.; Schroder, K.; White, H.; Fang, N. X.; Stoermer, M. J.; Abbenante, G.; Martin, J. L.; Young, P. R.; Fairlie, D. P. Activity of Recombinant Dengue 2 Virus NS3 Protease in the Presence of a Truncated NS2B Co-Factor, Small Peptide Substrates, and Inhibitors. *J. Biol. Chem.* **2001**, *276*, 45762–45771.
- (25) Holbeck, S. L.; Collins, J. M.; Doroshow, J. H. Analysis of FDA-Approved Anti-Cancer Agents in the NCI60 Panel of Human Tumor Cell Lines. *Mol. Cancer Ther.* **2010**, *9*, 1451–1460.
- (26) Dwivedi, V. D.; Tripathi, I. P.; Bharadwaj, S.; Kaushik, A. C.; Mishra, S. K. Identification of New Potent Inhibitors of Dengue Virus NS3 Protease from Traditional Chinese Medicine Database. *VirusDisease* **2016**, *27*, 220–225.
- (27) Othman, R.; Kiat, T. S.; Khalid, N.; Yusof, R.; Irene Newhouse, E.; Newhouse, J. S.; Alam, M.; Rahman, N. A. Docking of Noncompetitive Inhibitors into Dengue Virus Type 2 Protease: Understanding the Interactions with Allosteric Binding Sites. *J. Chem. Inf. Model.* **2008**, *48*, 1582–1591.
- (28) Hariono, M.; Choi, S. B.; Roslim, R. F.; Nawati, M. S.; Tan, M. L.; Kamarulzaman, E. E.; Mohamed, N.; Yusof, R.; Othman, S.; Rahman, N. A.; Othman, R.; Wahab, H. A. Thioguanine-Based DENV-2 NS2B/NS3 Protease Inhibitors: Virtual Screening, Synthesis, Biological Evaluation and Molecular Modelling. *PLoS One* **2019**, *14*, No. e0210869.
- (29) Katz, B. A.; Elrod, K.; Luong, C.; Rice, M. J.; Mackman, R. L.; Sprengeler, P. A.; Spencer, J.; Hataye, J.; Janc, J.; Link, J.; Litvak, J.; Rai, R.; Rice, K.; Sideris, S.; Verner, E.; Young, W. A Novel Serine Protease Inhibition Motif Involving a Multi-Centered Short Hydrogen Bonding Network at the Active Site. *J. Mol. Biol.* **2001**, *307*, 1451–1486.
- (30) Schmidtke, P.; Barril, X. Understanding and Predicting Druggability. A High-Throughput Method for Detection of Drug Binding Sites. *J. Med. Chem.* **2010**, *53*, 5858–5867.
- (31) Gaulton, A.; Hersey, A.; Nowotka, M.; Bento, A. P.; Chambers, J.; Mendez, D.; Motow, P.; Atkinson, F.; Bellis, L. J.; Cibrián-Uhalte, E.; Davies, M.; Dedman, N.; Karlsson, A.; Magariños, M. P.; Overington, J. P.; Papadatos, G.; Smit, I.; Leach, A. R. The ChEMBL Database in 2017. *Nucleic Acids Res.* **2017**, *45*, D945–D954.
- (32) Kim, S.; Chen, J.; Cheng, T.; Gindulyte, A.; He, J.; He, S.; Li, Q.; Shoemaker, B. A.; Thiessen, P. A.; Yu, B.; Zaslavsky, L.; Zhang, J.; Bolton, E. E. PubChem 2019 Update: Improved Access to Chemical Data. *Nucleic Acids Res.* **2019**, *47*, D1102–D1109.
- (33) Liu, T.; Lin, Y.; Wen, X.; Jorissen, R. N.; Gilson, M. K. BindingDB: A Web-Accessible Database of Experimentally Determined Protein-Ligand Binding Affinities. *Nucleic Acids Res.* **2007**, *35*, D198–D201.
- (34) The UniProt Consortium. UniProt: A Worldwide Hub of Protein Knowledge. *Nucleic Acids Res.* **2019**, *47*, D506–D515.
- (35) Rogers, D.; Hahn, M. Extended-Connectivity Fingerprints. *J. Chem. Inf. Model.* **2010**, *50*, 742–754.
- (36) Bender, A. How Similar Are Those Molecules after All? Use Two Descriptors and You Will Have Three Different Answers. *Expert Opin. Drug Discovery* **2010**, *5*, 1141–1151.
- (37) Parzen, E. On Estimation of a Probability Density Function and Mode. *Ann. Math. Stat.* **1962**, *33*, 1065–1076.
- (38) Rosenblatt, M. Remarks on Some Nonparametric Estimates of a Density Function. *Ann. Math. Stat.* **1956**, *27*, 832–837.
- (39) Aitchison, J.; Aitken, C. G. G. Multivariate Binary Discrimination by the Kernel Method. *Biometrika* **1976**, *63*, 413–420.
- (40) Edgar, R. C. MUSCLE: Multiple Sequence Alignment with High Accuracy and High Throughput. *Nucleic Acids Res.* **2004**, *32*, 1792–1797.
- (41) Grant, B. J.; Rodrigues, A. P. C.; ElSawy, K. M.; McCammon, J. A.; Caves, L. S. D. Bio3d: An R Package for the Comparative Analysis of Protein Structures. *Bioinformatics* **2006**, *22*, 2695–2696.
- (42) Mathea, M.; Klingspohn, W.; Baumann, K. Chemoinformatic Classification Methods and Their Applicability Domain. *Mol. Inf.* **2016**, *35*, 160–180.
- (43) Afantitis, A.; Melagraki, G.; Sarimveis, H.; Koutentis, P. A.; Markopoulos, J.; Igglessi-Markopoulou, O. Development and Evaluation of a QSPR Model for the Prediction of Diamagnetic Susceptibility. *QSAR Comb. Sci.* **2008**, *27*, 432–436.
- (44) Melagraki, G.; Afantitis, A.; Sarimveis, H.; Koutentis, P. A.; Kollias, G.; Igglessi-Markopoulou, O. Predictive QSAR Workflow for the in Silico Identification and Screening of Novel HDAC Inhibitors. *Mol. Diversity* **2009**, *13*, 301–311.
- (45) Berthold, M. R.; Cebron, N.; Dill, F.; Gabriel, T. R.; Kötter, T.; Meinl, T.; Ohl, P.; Sieb, C.; Thiel, K.; Wiswedel, B. KNIME: The Konstanz Information Miner. In *Data Analysis, Machine Learning, and Applications*; Preisach, C.; Burkhardt, H.; Schmidt-Thieme, L.; Decker, R., Eds.; Springer: Berlin Heidelberg, 2008; pp 319–326.
- (46) Zandi, K.; Teoh, B.-T.; Sam, S.-S.; Wong, P.-F.; Mustafa, M. R.; AbuBakar, S. Novel Antiviral Activity of Baicalein against Dengue Virus. *BMC Complementary Altern. Med.* **2012**, *12*, No. 214.
- (47) Rothan, H. A.; Abdulrahman, A. Y.; Sasikumer, P. G.; Othman, S.; Abd Rahman, N.; Yusof, R. Protegrin-1 Inhibits Dengue NS2B-NS3 Serine Protease and Viral Replication in MK2 Cells. *J. Biomed. Biotechnol.* **2012**, *2012*, 1–6.
- (48) The PyMOL Molecular Graphics System, Version 2.0; Schrödinger, LLC, 2017.
- (49) Valdés-Tresanco, M. S.; Valdés-Tresanco, M. E.; Valiente, P. A.; Moreno, E. AMDock: A Versatile Graphical Tool for Assisting Molecular Docking with Autodock Vina and Autodock4. *Biol. Direct* **2020**, *15*, No. 12.
- (50) Dolinsky, T. J.; Nielsen, J. E.; McCammon, J. A.; Baker, N. A. PDB2PQR: An Automated Pipeline for the Setup of Poisson–Boltzmann Electrostatics Calculations. *Nucleic Acids Res.* **2004**, *32*, W665–W667.
- (51) Trott, O.; Olson, A. J. AutoDock Vina: Improving the Speed and Accuracy of Docking with a New Scoring Function, Efficient Optimization, and Multithreading. *J. Comput. Chem.* **2010**, *31*, 455–461.
- (52) *Discovery Studio Visualizer*, v21.1.0.20298; Biovia, Dassault Systemes: San Diego, 2021.
- (53) Maia, W. M. N.; de Andrade, F. D. C. P.; Filgueiras, L. A.; Mendes, A. N.; Assunção, A. F. C.; Rodrigues, N. D. S.; Marques, R. B.; Filho, A. L. M. L.; de Sousa, D. P.; Da Silva Lopes, L. Antidepressant Activity of Rose Oxide Essential Oil: Possible Involvement of Serotonergic Transmission. *Heliyon* **2021**, *7*, No. e06620.
- (54) Siramshetty, V. B.; Grishagin, I.; Nguyen, Đa.-T.; Peryea, T.; Skovpen, Y.; Stroganov, O.; Katzel, D.; Sheils, T.; Jadhav, A.; Mathe, E. A.; Southall, N. T. NCATS Inxight Drugs: A Comprehensive and Curated Portal for Translational Research. *Nucleic Acids Res.* **2022**, *50* (D1), D1307–D1316.
- (55) Raghavan, S.; Rajendar, S. Stereoselective Total Synthesis of (–)-Nupharamine Utilizing an α -Chlorosulfide and a Sulfinimine for C–C Bond Formation. *Org. Biomol. Chem.* **2016**, *14*, 131–137.
- (56) American Chemical Society. Diaboline, 2022. <https://www.acs.org/content/acs/en/molecule-of-the-week/archive/d/diaboline.html>. (accessed July 26, 2022).
- (57) Russo, E. B.; Marcu, J. Cannabis Pharmacology: The Usual Suspects and a Few Promising Leads. In *Cannabinoid Pharmacology*; Kendall, D.; Alexander, S. P. H., Eds.; Academic Press, 2017; Vol. 8, pp 67–134.